Laser wavelength metrology with color sensor chips

Tyler B. Jones,[1] Nils Otterstrom,[1] Jarom Jackson,[1] James Archibald,[1,2] and Dallin S. Durfee[1,*]

[1]*Department of Physics and Astronomy, Brigham Young University, USA*
[2]*AMS-TAOS USA Inc., USA*
[*]*dallin_durfee@byu.edu*

Abstract: We present a laser wavelength meter based on a commercial color sensor chip. The chip consists of an array of photodiodes with different absorptive color filters. By comparing the relative amplitudes of light on the photodiodes, the wavelength of light can be determined. In addition to absorption in the filters, etalon effects add additional spectral features which improve the precision of the device. Comparing the measurements from the device to a commercial wavelength meter and to an atomic reference, we found that the device has picometer-level precision and picometer-scale drift over a period longer than a month.

OCIS codes: (120.3940) Metrology; (330.1710) Color, measurement; (350.2460) Filters, interference; (230.0040) Detectors.

References and links

1. V. C. Coffey, "Wavelength meters: How to select a wavelength meter," LFW (2009). Retrieved 9/17/2015.
2. T. Udem, R. Holzwarth, and T. W. Hänsch, "Optical frequency metrology," Nature **416**, 233–237 (2002).
3. J. Ishikawa, N. Ito, and K. Tanaka, "Accurate wavelength meter for cw lasers," Appl. Opt. **25**, 639–643 (1986).
4. N. Konishi, T. Suzuki, Y. Taira, H. Kato, and T. Kasuya, "High precision wavelength meter with Fabry-Perot optics," Appl. Phys. **25**, 311–316 (1981).
5. "Bristol 521 series specification sheet," Tech. rep., Bristol Instruments (2015).
6. "Ocean optics HR4000 specifications," Tech. rep., Ocean Optics (2015).
7. J. D. White and R. E. Scholten, "Compact diffraction grating laser wavemeter with sub-picometer accuracy and picowatt sensitivity using a webcam imaging sensor," Rev. Sci. Instrum. **83**, 113104 (2012).
8. R. F. Nabiev, C. J. Chang-Hasnain, L. E. Eng, and K.-Y. Lau, "Monolithic wavelength meter and photodetector using a wavelength dependent reflector," U.S. Patent **5,760,419** (1998).
9. M. Muneeb, A. Ruocco, A. Malik, S. Pathak, E. Ryckeboer, D. Sanchez, L. Cerutti, J. Rodriguez, E. Tournié, W. Bogaerts, M. K. Smit, G. Roelkens, "Silicon-on-insulator shortwave infrared wavelength meter with integrated photodiodes for on-chip laser monitoring," Opt. Express **22**, 27300–27308 (2014).
10. P. Fox, R. Scholten, M. Walkiewicz, and R. Drullinger, "A reliable, compact, and low-cost Michelson wavemeter for laser wavelength measurement," Am. J. Phys. **67**, 624–630 (1999).
11. B. Redding, S. M. Popoff, and H. Cao, "All-fiber spectrometer based on speckle pattern reconstruction," Opt. Express **21**, 6584–6600 (2013).
12. S. Roy, S. Chaudhuri, and C. Unnikrishnan, "A simple and inexpensive electronic wavelength-meter using a dual-output photodiode," Am. J. Phys. **73**, 571–573 (2005).
13. "TCS3414 datasheet," Tech. rep., ams AG (2011).
14. J. J. Snyder, "Fizeau wavelength meter," Laser Spectroscopy III **IX**, 419–420 (1977).
15. F. Bitte and T. Pfeifer, "Alternative methods for wavelength determination: interference filters and double photodiodes," Proc. SPIE **3823**, 20–25 (1999).

#252564 Received 23 Oct 2015; revised 26 Nov 2015; accepted 26 Nov 2015; published 9 Dec 2015

1. Introduction

Precise wavelength measurements of lasers and other narrow-band light sources are critical for many applications, such as laser spectroscopy and laser cooling and trapping. A variety of commercial devices, with different precisions and advantages, are used to measure wavelength [1]. These include optical frequency combs with sub-femtometer precision [2], interferometric wavelength meters which often have sub-picometer (pm) precision [3–5], and grating spectrometers, which typically have less precision, but can provide a complete spectral curve [6]. In addition, many other devices as well as variants of these have been researched (see, for example [7–12]). These devices typically require precise alignment. Some involve moving parts or lasers which limit lifetime or require regular maintenance. The cost of commercial devices typically ranges from thousands to tens or even hundreds of thousands of dollars.

We have developed a small, robust, and inexpensive wavelength meter based on a commercial color sensor chip. While this chip was designed for applications involving broad-band light, such as color balancing of TV and cell phone displays and cameras [13], we have been able to use the device to determine the wavelength of single-frequency lasers with an accuracy of a few picometers with picometer-level drift over month-long time scales. The device consists of the color sensor chip, electronics (including a microcontroller and a temperature controller), a small Peltier cooler mounted to a small copper plate, a single-mode optical fiber, and an enclosure. While wavelength calculations could be performed on a microcontroller, for our experiments we recorded raw data and performed calculations offline on a personal computer.

The device could be used instead of more expensive and fragile wavelength meters for many applications in atomic physics labs or in teaching labs. Its size, simplicity, low power requirements, and its ability to withstand mechanical shock could make it useful for portable systems or systems which must be exposed to the environment. The low cost and small size of the device could help make mass-produced spectroscopic consumer devices possible. It is possible that greater precision and stability could be achieved by modification of our design for greater mechanical and thermal stability. And it is possible that using other color sensor chips, or a discrete set of photodiodes, possibly using a larger number of different absorptive filters, could improve performance.

2. The color sensor

The color sensor chip that we used, the TCS3414 from AMS, has an 8x2 array of 16 photodiodes arranged in a 1.57×0.35 mm rectangle, each covered with either a red, green, blue, or clear absorptive filter. It comes in two package styles - a 2×2 mm "CS" package, and a 3×3 mm "FN" package. The CS package has an additional IR-blocking filter, such that the spectral response curves of the diodes are different for the two packages. Each group of photodiodes (which we will refer to as the red, green, blue, and clear channels) is connected to an analog to digital converter which converts the photocurrent from the channel, integrated over a fixed time, to a digital number. From these numbers, the intensity and color of light can be determined.

The TCS3414 color sensor chip was designed to measure broadband light, and only two specifications related to its potential to measure the wavelength of a narrow-band source are published in its datasheet [13]; the temperature coefficient for the responsivity of the individual detectors is indicated to be 200 parts per million (ppm) per degree Celsius, and the bit depth of the digitizers was stated to be 16 bits. Using response curves for the different color channels given in the datasheet [13] we estimated that a 200 ppm drift in any single color channel would result in errors less than 10 pm for most wavelengths from 350 to 800 nm, and less than 20 pm for all wavelengths in that range except for a band from 450 to 465 and a small band near 715 nm.

When we tested the temperature coefficient using a single-frequency red laser, we found it

#252564 Received 23 Oct 2015; revised 26 Nov 2015; accepted 26 Nov 2015; published 9 Dec 2015

to be much larger than 200 ppm/°C. As shown in Fig. 1, both FN and CS packages exhibit a sinusoidal response as the temperature of the sensor is changed, suggesting that surfaces in the window/filter assemblies form etalons, resulting in interference. We saw similar variations when scanning the wavelength of the laser while holding the temperature constant. Since etalon effects are washed out when using broadband light, it is not surprising that the datasheet doesn't mention this phenomena or its effect on the temperature coefficient.

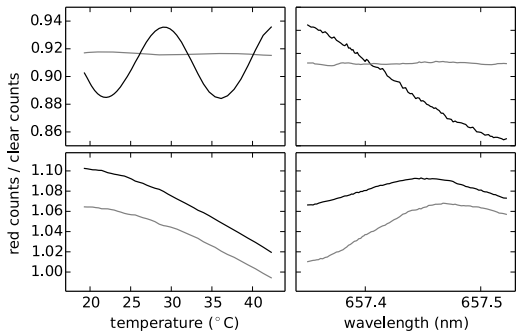

Fig. 1. Etalon effects in the color sensors. The plots show the number of counts measured on the red channel normalized to the number of counts on the clear channel. For the plots on the left, this ratio is plotted as a function of the temperature of the color sensors while the wavelength of the laser is held constant. For the plots on the right, the ratio is plotted as a function of the wavelength of the laser as the temperature is held constant. The upper plots were made using FN-package sensors, and the lower plots using CS-package sensors. The data points represented by the gray lines were taken using a sensor that had been sanded in an attempt to randomize reflections off of the first surface of the detector. The data points represented by the black lines were taken using an unsanded sensor. Ratios larger than one are likely due to a maximum in the etalon transmission for the red channel occurring at nearly the same wavelength as a minimum etalon transmission for the clear channel.

The dominant etalon effects are different for the two packages. As seen in Fig. 1, the free spectral range for the fringes is different for the FN and CS packages. Also, the etalon effects in the FN package can be removed by sanding the surface of the window over the photodiode array to randomize reflection angles. Sanding the window did not affect etalon effects in the CS package.

Without sufficient temperature control, etalon effects could significantly impair the long-term stability of the device. However, if temperature is well controlled, small-scale spectral features introduced by the interference makes it possible to more accurately distinguish between similar wavelengths, making this device similar to wavelength meters based on Fizeau interferometers [14] or interference filters [15]. Based on the data in Fig. 1, temperature control at the 0.4°C level should be sufficient for picometer stability using the CS package, while better than 0.2°C stability would be required for the FN package.

We found that with simple temperature control, we could take advantage of the etalon fringes in the CS package to achieve excellent wavelength discrimination and good long-term stability (we had less success with the FN package, with either a sanded or an un-sanded window). Since all photodiodes with a given type of color filter are summed together, it is possible that etalon effects in one photodiode could partially cancel effects in different photodiodes. Also, since the thickness variations in the windows and filters on the photodiodes are presumably random, one would expect that performance would be somewhat different from chip to chip. In fact, chip to chip variations of etalon effects makes the spectral response of a given color channel slightly

#252564 Received 23 Oct 2015; revised 26 Nov 2015; accepted 26 Nov 2015; published 9 Dec 2015

different in two different chips, such that by making measurements using multiple CS package chips simultaneously one can gain additional information about the measured wavelength. While we have chosen to present data from a single chip in this paper, by combining data taken from a second chip present in our apparatus, we sometimes found a small improvement in the accuracy of the device. We have yet to explore the possibility of using an array of many chips.

To control the temperature of the color sensor, the circuit board on which the sensor was mounted was attached to a copper plate with a thin electrical insulator between them. A thermoelectric cooler was then sandwiched between the copper plate and the aluminum box in which the sensor was mounted. This way the aluminum box served as a heat sink for the cooler. A thermistor was attached to the copper plate, and a Thorlabs TEC 2000 temperature controller was used to drive current through the cooler to keep the temperature fixed at the location of the thermistor. This particular temperature controller was selected simply because it was available in our lab and not being used. However, based on the data in figure 1, a much simpler controller should suffice - either a simple analog controller made from opamps and a mosfet, or a simple digital controller made using the same inexpensive microcontroller used to control the color sensor.

The 16-bit analog to digital converters place a 15 ppm upper limit on the accuracy of the photodiode readings. This is sufficient for wavelength measurements at the pm level as long as light levels are large enough to take advantage of most of the digitizer's bit depth. Calculations based on the response curves at the wavelengths used in this study indicated that if the lowest value in any channel was above 1000 counts, picometer accuracy could be achieved. For low light levels, integration times can be lengthened to increase counts. For higher light levels, integration times must be reduced to prevent saturation of the digitizer. For our experiments, in which a few mW of light was coupled to the device, integration times from 50 to 200 ms were used.

We experimented with using multiple integration times for a single measurement - using a short integration time to get readings for color channels with high counts, and a longer integration time which saturated some channels but gave higher resolution readings on channels with smaller signals. A channel which received an intermediate amount of light was used to scale the readings to account for imperfect timing on the integration and possible fluctuations in laser intensity between the readings. For example, when making measurements of a 461 nm blue laser with an integration time that resulted in the clear channel being near saturation, the green channel read just over 5000 counts and the red channel read just over 1000 counts. By increasing the integration time such that the clear and blue channels saturate, but the green channel is just below saturation, it's possible to get a second reading with more bit resolution on the red channel, and the green channel can be used to scale the reading to connect it to the first reading at a shorter integration time. We did not use this technique for the results presented in this paper, however, because it did not result in significant improvement in our measurements.

The relative size of the signals from the red, green, blue, and clear channels depends on the spatial distribution of the light hitting the sensor. For example, if light from a blue laser is focused on a single red-filtered photodiode, the sensor will record mostly red counts, leading to the erroneous conclusion that the laser light is red. To ensure a relatively even and consistent illumination of the photodiode array, laser light is coupled into a Thorlabs PM-S405-XP single-mode optical fiber, and the light exiting the fiber is allowed to spread before striking the sensor which is 16 cm away. The fiber has a nominal numerical aperture of 0.12, producing an approximate Gaussian profile with a radius of about 2 cm at the location of the sensor, resulting in an illumination pattern which is fairly uniform and very stable. The end of the fiber is attached to one side of the aluminum box housing the sensor, and the color sensor is attached to the opposite side, keeping the fiber/sensor alignment fixed. The box also serves to block any

#252564 Received 23 Oct 2015; revised 26 Nov 2015; accepted 26 Nov 2015; published 9 Dec 2015

ambient light; using our standard integration times, the sensor detects no light on any of the channels when the laser is turned off.

3. Determining the wavelength

To determine the wavelength of light hitting the color sensor, we read the digitized light signals using an Arduino microcontroller. To make a measurement, the microcontroller sends a command to begin integrating the light signal. It then waits a predetermined integration time based on the light level (typically between 50 and 200 ms in our experiments), allowing the signal on the clear channel to integrate near to, but not beyond, the 16-bit saturation point. The microcontroller then issues a command to stop integrating the light signal and then reads out the 16-bit value from each of the four color channels.

To calibrate the device, part of a laser beam is split off and coupled into the device through the optical fiber. Another part of the beam is sent to a Bristol 521 commercial wavelength meter which serves as a reference. The computer then scans the laser in a random pattern over its tuning range. At each laser setting, the laser is first allowed to settle for several seconds, and then several readings are taken from both the color sensor and the commercial wavelength meter.

To reduce sensitivity to light intensity, each of the channel signals is normalized by dividing by the sum of the signals from each channel. For example, if the digital number read from the four channels at a given wavelength are denoted as $r(\lambda)$, $g(\lambda)$, $b(\lambda)$, and $c(\lambda)$, the normalized value for the red channel, $R(\lambda)$, is given by

$$R(\lambda) = \frac{r(\lambda)}{r(\lambda)+g(\lambda)+b(\lambda)+c(\lambda)}. \tag{1}$$

One could also, conceivably, normalize to the clear channel. But, because of the etalon effects, the clear channel is not simply a measure of the laser intensity, but is essentially equivalent to the other channels in its function in determining the laser wavelength. As such, we chose to use a normalization which was symmetric with respect to all of the channels.

The normalized outputs of each of the four color channels, as a function of wavelength measured by the commercial meter, are then fit to either a sine wave plus a second-order polynomial or, if the fitting routine (curve_fit from Python's scipy.optimize package) doesn't find a good fit to the sine wave, to an eighth-order polynomial. The curve fit parameters are then saved. In addition, a fit error for each color channel is calculated by calculating the rms average of the residual, normalized to the total range of values in the fit. These fit errors allow us to give more weight to color channels with better fits when using the device to determine the wavelength of a laser. The curve fit parameters and the fit errors constitute the calibration of the device.

To determine the unknown wavelength of a laser, the light signal is integrated, and then the four color channels are read. The signals are normalized to the sum of the signals from all color channels. We denote the normalized signals as R, G, B, and C. From these values, a channel-specific "confidence" function is calculated by taking the square of the fractional difference between the normalized signal on each channel and the value given by that channel's calibration curve as a function of wavelength. For example, if the curve fit for the red channel is denoted as $f_r(\lambda)$, the red channel confidence function is given by

$$C_r(\lambda) = \left(\frac{f_r(\lambda)-R}{f_r(\lambda)}\right)^2. \tag{2}$$

Each of the channel-specific confidence curves are then weighted by one over the fit error for the channel squared, and the curves for all four color channels are summed to produce an overall

#252564 Received 23 Oct 2015; revised 26 Nov 2015; accepted 26 Nov 2015; published 9 Dec 2015

confidence function. If the calibration fit errors for the red, green, blue, and clear channels are written as er_r, er_g, er_b, and er_c, respectively, the overall confidence function has the form

$$C(\lambda) = \frac{C_r(\lambda)}{er_r^2} + \frac{C_g(\lambda)}{er_g^2} + \frac{C_b(\lambda)}{er_b^2} + \frac{C_c(\lambda)}{er_c^2}. \tag{3}$$

The wavelength is determined to be the point at which this confidence function is minimized. An example of the confidence curves for several measurements we made is shown in Fig. 2.

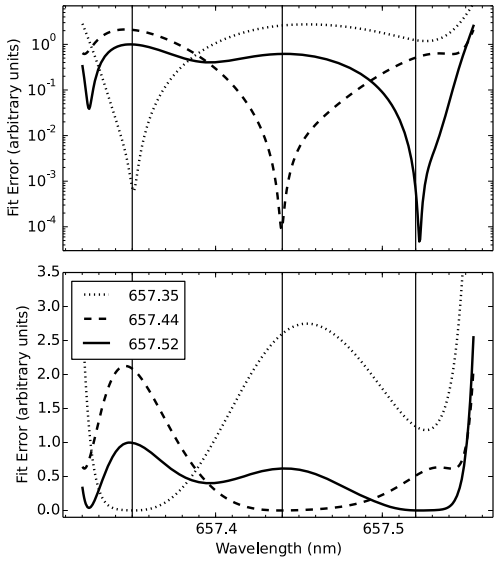

Fig. 2. Determining the wavelength. The confidence curve, calculated by taking differences from the measured value and the calibration curves for each color channel as a function of wavelength, is shown for measurements of a laser beam at three different wavelengths. The curves are shown on a semi-log (upper) and linear (lower) scale. The vertical black lines indicate the laser wavelength determined by the commercial wavelength meter for the three measurements.

We experimented with different ways to weight the different channels. Giving greater weight to parts of the calibration curves with larger derivatives resulted in little change in accuracy. A small but noticeable improvement was found when we weighted each channel with the size of the measured signal for that channel, such that the fit favored data with less bit noise. A more noticeable improvement was found when we weighted using the residuals from the calibration curve fits, as described above, such that higher weighting was given to channels with better calibration fits.

As can be seen in the linear-scale plot in Fig. 2, the confidence curves tend to have very shallow minima. However, as seen in the log-scale plot, the noise is sufficiently small to determine the minimum with picometer-scale precision. Also note that the curves have multiple local minima. This is particularly noticeable on the 657.52 nm curve. This is due to the periodic nature of etalon transmission. The absorptive properties of the filters change quickly enough on this scale that we can clearly determine which is the true minimum. This implies that it should be possible to calibrate the device and determine wavelengths over a very wide range of wavelengths, though we were unable to test this due to the limited scanning ranges of our lasers. However, due to the flat minima and the periodic local minima, discrimination of the correct

#252564 Received 23 Oct 2015; revised 26 Nov 2015; accepted 26 Nov 2015; published 9 Dec 2015

etalon order requires clean signals. For a few experiments in which readings were noisier (possibly due to a loose fiber mount or an unstable laser that wasn't operating completely in a single mode) there was a greater spread in wavelength readings, and in these experiments, often the spread of readings for a laser at a given wavelength would be bimodal.

Assuming that the color sensor's response is linear, the signal normalizing done in the curve fitting algorithm should result in accuracy which is not significantly affected by light intensity. To verify this, we first calibrated our sensor, and then, with the laser's wavelength fixed, we measured the change in wavelength determined by our algorithm while changing the amount of light coupled into the optical fiber. We found that when we varied the power from 500 to 1400 μW, the measured wavelength varied by less than 1 pm.

The algorithm inherently assumes that the laser has a negligible linewidth compared to the accuracy of the device. This is a reasonable assumption for a typical single-frequency laser. We numerically studied what would happen for light with a broader linewidth using measured calibration curves generated by scanning a red single-frequency diode laser. For either a Gaussian or Lorentzian line with a full-width half-maximum linewidth of 100 pm centered at 657.4 nm, the algorithm found the center of the line to within 2 pm. Presumably accuracy would decrease significantly if the linewidth was on the order of or larger than the free spectral range of the etalons. We cannot test this directly because our lasers cannot scan sufficiently far to generate the calibration curves needed.

4. Results

We took several sets of data using two different single-frequency diode lasers to determine the accuracy and long-term stability of the device. As mentioned above, we achieved the best results using the CS package color sensor. All of the data sets presented here were taken using a CS package sensor.

For one data set we took measurements at various wavelengths produced by a red laser (a New Focus Vortex 6000 ECDL laser) over a span of over a month. The first five hours of this data set were used to calibrate the device, as described above. When taking this data, every few seconds the grating piezo voltage on the laser was set to a new random value to change the wavelength of the laser. After allowing the laser wavelength to settle for six seconds, 20 wavelength readings were rapidly taken from both our device and the commercial wavelength meter at a rate of about four readings every second. After the 20 readings, the laser piezo voltage was changed, changing the wavelength of the laser, and the process was repeated. During the experiment the laser was repeatedly scanned randomly over the entire ~ 0.18 nm wavelength range of the laser.

The measurement error was inferred by taking the difference in the measured wavelength and the wavelength measured by the commercial meter. The wavelength error is plotted as a function of time as trace (a) in Fig. 3. The gap in this data set was due to a problem with the commercial wavelength meter such that for a period of a few days we don't have reference measurement to which we can compare measurements from our device. The error as function of wavelength at various times during this experiment is shown in Fig. 4. This experiment was performed in an active lab - with people regularly working on experiments near the laser and the device.

Traces (b) and (c) in Fig. 3 are two data sets taken by locking a blue diode laser (a New Focus TLB 6700 ECDL laser) to the 461 nm atomic resonance in strontium. In these experiments we first scanned the laser over its entire ~ 0.1 nm range to generate a calibration curve. Then the laser was locked and wavelength measurements were taken rapidly. This allowed us to measure the drift in our instrument independent of the commercial wavemeter. It reduced potential errors due to laser drift while measurements are being made, especially drifts between the time that the

#252564 Received 23 Oct 2015; revised 26 Nov 2015; accepted 26 Nov 2015; published 9 Dec 2015

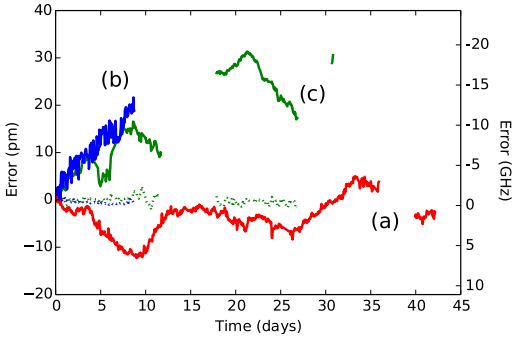

Fig. 3. Calibration drift as a function of time for several long data sets. Lines (a), (b), and (c) show the difference of the wavelength measured by our device from the actual wavelength of the laser as a function of time. The readings from the commercial meter that go along with the data sets (b) and (c) are plotted as dotted lines. To reduce the number of points plotted, measurements were averaged into bins an hour in length. The second y axis gives the drift of the laser frequency in GHz. Because the conversion from wavelength to frequency error is dependent on the exact wavelength, the scale was calculated using the formula $df = -(c/\lambda^2)d\lambda$, using a wavelength λ of 657.45 nm. Because both the scan range of the laser and the drifts are small, the GHz scale, while approximate, is quite accurate for the data taken with the red laser. Labels on the GHz scale should be multiplied by 2.03 for data taken with the blue laser.

wavelength is measured by our device and when it is measured by the commercial wavemeter. Also, by not changing the wavelength of the laser between measurements, we were able to take measurements faster to observe the noise and drift in our device at shorter time scales. This technique also allowed us to characterize the drift in the commercial wavemeter for these experiments. This drift for both data sets is shown in the figure for comparison. The gaps in data set (c) are due to a bug in the microcontroller software that caused it to crash.

The accuracy and drift over a wide range of time scales is illustrated in Fig. 5, which shows the Allan deviance for the data sets shown in Fig. 3. From this plot it can be seen that the short-time performance of the device even exceeds that of the commercial wavelength meter, and the deviation after 200 hours is just a few pm. Because of the time taken to change the wavelength of the laser and to wait for it to settle between measurements, for the experiment with the red laser no deviance could be calculated from this data set for times less than 25 seconds. For the data sets using the blue laser locked to an atomic transition we could calculate deviations for times less than one second.

All data sets show picometer or sub-picometer deviations over all of the time scales measured. We speculate that the difference between line (b) and (c) for time scales from 10^{-3} to 10^{1} hours could be due to the fact that the fiber mount had come loose, and was re-tightened before taking data set (c). The higher deviation at short time scales and lower deviation at longer time scales for data set (a), relative to the other two, could be a related to the different wavelength used. It is more likely, however, that the higher deviation at short time scales is mainly due to the fact that, since the laser wasn't locked, there was more drift between the times that the wavelength was measured with our device and when it was measured by the reference commercial wavelength meter.

#252564 Received 23 Oct 2015; revised 26 Nov 2015; accepted 26 Nov 2015; published 9 Dec 2015

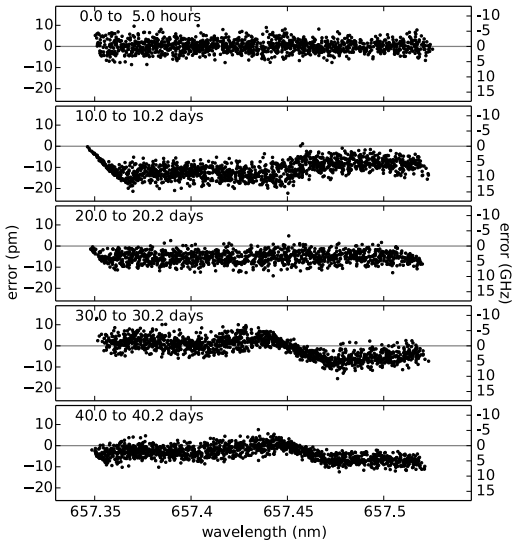

Fig. 4. Error as a function of wavelength for a long data set. The same data plotted in line (a) on Fig. 3 is plotted here as a function of the wavelength measured by the commercial meter. Each point in each plot is the average of the 20 measurements made at a particular laser piezo voltage. In the top-most plot, the data points taken during the first five hours of the data are shown. These are the data points which were used to calibrate the device for this experiment. The other plots each show a 5-hour long segment of data starting 10, 20, 30, and 40 days into the experiment. The second *y* axis gives the drift of the laser frequency in GHz. Because the conversion from wavelength to frequency error is dependent on the exact wavelength, the scale was calculated using the formula $df = -(c/\lambda^2)d\lambda$, using a wavelength λ of 657.45 nm. Because both the scan range of the laser and the drifts are small, the GHz scale, while approximate, is quite accurate.

5. Conclusions

We have shown that a commercial color sensor chip can be used to measure the wavelength of a narrow-band light source, such as a laser, with picometer precision, with picometer-scale drifts over the time scale of a month. Because these chips are mass produced for consumer electronics, devices using them could be made at very low cost. Such a device can be extremely robust and very small, and could operate on very low power. Such a device could be used in portable spectroscopy experiments or spectroscopic devices which must be exposed to the elements, student optics labs, and consumer applications.

Future work on this device could include evaluation of drift over much longer time scales, and temperature cycling to simulate aging. It would also be important to determine performance over a wider range of wavelengths, both to determine if there are wavelengths at which the device doesn't perform as well and to determine how well the device can discriminate the wavelength when searching for the minimum in the confidence function over a much wider range of wavelengths. It is possible that improvement of fiber mount rigidity could improve stability. A more careful measurement of how temperature control affects stability should be done, and it would be interesting to see if it is possible to achieve stability without temperature control by measuring and compensating for temperature changes. Future work could also include testing more samples of the color sensor or different brands or models of color sensors (including sensors with more color channels), and testing how much combining simultaneous

#252564 Received 23 Oct 2015; revised 26 Nov 2015; accepted 26 Nov 2015; published 9 Dec 2015

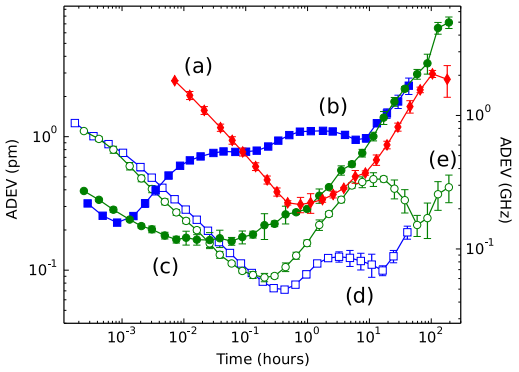

Fig. 5. Allan deviance. The Allan deviance for the data shown in Fig. 3 is plotted. Lines (a), (b), and (c) were calculated from the data shown in lines (a), (b), and (c) in Fig. 3. Plots (d) and (e) were calculated from the wavelengths measured using the commercial wavemeter at the same time data sets (b) and (c) were taken, respectively. Unlike Fig. 3, the data was not averaged prior to calculating the Allan deviances. Once the Allan deviance curves were calculated, deviance data was grouped and averaged to make the points shown on the plots. The standard deviation of the Allan deviation within groups is shown as error bars on each plot. The second *y* axis gives the drift of the laser frequency in GHz. Because the conversion from wavelength to frequency error is dependent on the exact wavelength, the scale was calculated using the formula $df = (c/\lambda^2)d\lambda$, using a wavelength λ of 657.45 nm. Because both the scan range of the laser and the drifts are small, the GHz scale, while approximate, is quite accurate for the data taken with the red laser. Labels on the GHz scale should be multiplied by 2.03 for data taken with the blue laser.

measurements from a number of chips can improve precision.

Acknowledgments

We would like to acknowledge funding from NSF grant number PHY-1205736 and from Brigham Young University's College of Physical and Mathematical Science. We would also like to acknowledge the assistance of Kevin Blissett.

#252564 Received 23 Oct 2015; revised 26 Nov 2015; accepted 26 Nov 2015; published 9 Dec 2015